Laser control of molecular photodissociation with use of the complete reflection phenomenon

Kuninobu Nagaya
Department of Functional Molecular Science, School of Mathematical and Physical Science,
The Graduate University for Advanced Studies, Myodaiji, Okazaki 444-8585, Japan

Yoshiaki Teranishi
RIKEN, Hirosawa 2-1, Wako 351-01, Japan

Hiroki Nakamura[a)]
Department of Functional Molecular Science, School of Mathematical and Physical Science,
The Graduate University for Advanced Studies, Myodaiji, Okazaki 444-8585, Japan and Department of
Theoretical Studies, Institute for Molecular Science, Myodaiji, Okazaki 444-8585, Japan

A new idea of controlling molecular photodissociation branching by a stationary laser field is proposed by utilizing the unusual intriguing quantum-mechanical phenomenon of complete reflection. By introducing the Floquet (or dressed) state formalism, we can artificially create potential curve crossings, which can be used to control molecular processes. Our control scheme presented here is summarized as follows. First, we prepare an appropriate vibrationally excited state in the ground electronic state, and at the same time by applying a stationary laser field of the frequency ω we create two nonadiabatic tunneling (NT) type curve crossings between the ground electronic bound state shifted up by one photon energy $\hbar\omega$ and the excited electronic state with two dissociative channels. In the NT-type of curve crossing where the two diabatic potential curves cross with opposite signs of slopes, it is known that the complete reflection phenomenon occurs at certain discrete energies. By adjusting the laser frequency to satisfy the complete reflection condition at the NT type curve crossing in one channel, the complete dissociation into the other channel can be realized. By taking one- and two-dimensional models which mimic the HOD molecule and using a wave packet propagation method, it is numerically demonstrated that a molecule can be dissociated into any desired channel selectively. Selective dissociation can be realized even into such a channel that cannot be achieved in the ordinary photodissociation because of a potential barrier in the excited electronic state. © *2000 American Institute of Physics.* [S0021-9606(00)00639-5]

I. INTRODUCTION

Recently, control of molecular processes or chemical reactions by laser fields has attracted much attention and has become a hot topic of science thanks to a remarkable progress of laser technology.[1,2] Several ideas have been proposed so far such as coherent control,[3] pump–dump method,[4] pulse-shape driven control,[5–8] and adiabatic rapid passage with use of the chirped pulse.[9–13] The essence of the coherent control method originated by Brumer and Shapiro[3] is to utilize the quantum mechanical interference effect to control the branching of a prepared state into possible decay channels with use of the phase and intensity of two laser pulses. The pump–dump scheme proposed by Tannor and Rice[4] is to prepare a localized wave packet on a bound electronic excited state with the first laser pulse (pump pulse) and make a transition to a final desirable state at some appropriate position with the second laser pulse (dump pulse). Pulse shape driven control to find the best laser pulse shapes to control wave packet dynamics (optimal control theory) has been formulated and discussed by Kosloff *et al.*,[5] Rabitz *et al.*,[6] Kohler *et al.*[7] and Fujimura *et al.*[8] The pulse shapes

are optimized under various restrictions. It is usually the case, however, that the optimized pulses have complicated structures in the laser frequency as well as in the laser amplitude. The use of a chirped (frequency-swept) laser pulse originally proposed by Chelkowski and Bandrauk[9] is also one of the effective methods and has been studied by many authors.[10–13] Most of them, however, utilize the so called adiabatic rapid passage (ARP), that is to say, the laser frequency is swept very slowly to keep the system on the same adiabatic state. Recently, a new scheme of control by sweeping laser frequency and/or laser intensity periodically has been proposed by Teranishi and Nakamura.[14,15]

As is well known, nonadiabatic transition due to potential curve crossing presents a very basic mechanism of state changes in various fields of physics, chemistry, and biology and always plays a crutial role in various molecular dynamic processes.[16,17] Molecular processes in laser fields can also be regarded as nonadiabatic transitions due to potential curve crossing, since the Floquet (or dressed) state formalism tells that curve crossings are created among the dressed states.[18] By choosing the laser frequency and/or intensity properly, those curve crossings may be manipulated to induce desirable nonadiabatic transitions. This is one of the most signifi-

---

cant features of laser control of molecular dynamic processes. In view of the importance of nonadiabatic transitions, we have proposed a new idea to control dynamic processes in a laser field by periodically sweeping the laser intensity and/or laser frequency at the avoided crossings among dressed states.[14,15] In this paper we propose another new idea based on the unusual intriguing quantum mechanical phenomenon of complete reflection, which occurs in the case of one-dimensional nonadiabatic tunneling (NT) type curve crossing. This phenomenon can be nicely treated and formulated by the semiclassical theory of nonadiabatic transitions recently completed by Zhu and Nakamura.[16,17,19,23] One- and two-dimensional models of photodissociation will be discussed for a triatomic molecule ABC consisting of a bound ground electronic state and a dissociative excited electronic state with two dissociation channels, A+BC and AB+C. In the one-dimensional model, complete and selective dissociation into any desired channel can be realized by adjusting the initial vibrational excited state and the laser frequency. In the two-dimensional case, the control cannot be complete but quite selective dissociation into any channel is possible. Even such a dissociation can be realized that a potential barrier hinders the ordinary photodissociation along the electronically excited state potential surface. The complete reflection phenomenon has been utilized to discuss the possibility of molecular switching in one- and two-dimensional arrays of the NT type potential units.[20–22] This is the first application of the phenomenon to laser control of photodissociation.

This paper is organized as follows. In Sec. II the physical explanation of the complete reflection phenomenon and the basic idea of our control scheme are presented with the help of the semiclassical theory of nonadiabatic transition. In Sec. III the basic idea is applied to the one-dimensional model and the completeness of our control scheme is numerically demonstrated by performing one-dimensional wave packet calculations. The numerical results are compared with the prediction by the semiclassical theory of Zhu–Nakamura. In Sec. IV two-dimensional systems based on the model potentials of the HOD molecule are treated numerically by using the two-dimensional wave packet propagation method. A comparison between the numerical results and the predictions from the one-dimensional theory is made, and favorable conditions for selective control of photodissociation branching are presented. Section V is devoted to concluding remarks.

II. COMPLETE REFLECTION IN NONADIABATIC TUNNELING TYPE TRANSITION AND BASIC IDEA OF CONTROL SCHEME

Let us first explain the complete reflection phenomenon, summarize the basic semiclassical theory to formulate the phenomenon and present briefly the basic idea of our control scheme with use of this phenomenon. In the case of NT type curve crossing in which the two diabatic potential curves cross with different signs of slopes [see Fig. 1(a)], the transmission probability at energies higher than the bottom of the upper adiabatic potential oscillates as a function of energy as is shown in Fig. 1(b). We note that there are following inter-
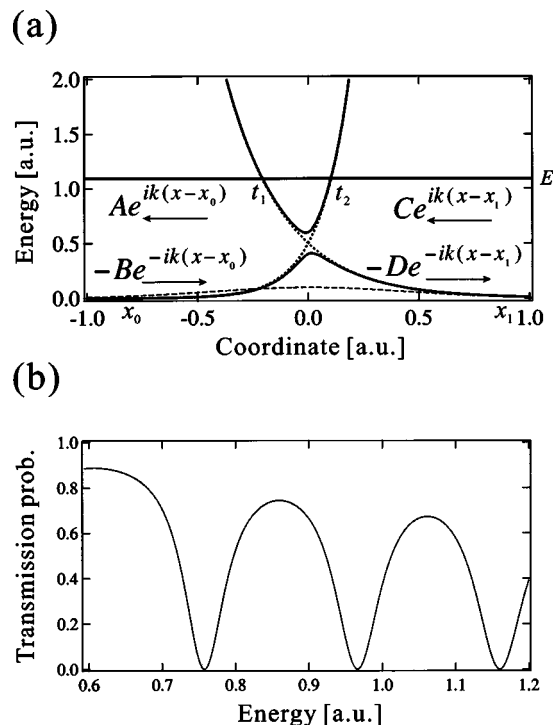
FIG. 1. (a) Schematic representation of the NT (nonadiabatic tunneling) type crossing potential. Solid (dotted) line: adiabatic (diabatic) potential. Dashed line: diabatic coupling. Potentials for $x \leq x_0$ and $x \geq x_1$ are assumed to be flat. (b) Transmission probability against energy for the potential of Fig. 1(a).

esting features: (i) The transmission probability dips always reach to zero, namely complete reflection is realized. (ii) This occurs irrespective of the shapes of potentials. (iii) The envelope of the probability decreases monotonically as energy increases. The semiclassical theory completed by Zhu and Nakamura furnishes the complete set of analytical formulas to describe the process.[16,17,19,23] The transmission amplitude T is given by

$$T \equiv |T|e^{i\delta_T} = \left[\frac{4\cos^2\psi}{4\cos^2\psi + p^2/(1-p)} \right]^{1/2} e^{i\delta_T} \tag{2.1}$$

with

$$\delta_T = \int_{x_0}^{x_1} k_1(x)dx + \sigma - \tan^{-1}\left[\frac{(1-p)\sin(2\psi)}{1+(1-p)\cos(2\psi)} \right] + \pi\Theta[-\text{sgn}(\cos\psi)], \tag{2.2}$$

where p and ψ represent, respectively, the nonadiabatic transition probability for one passage of the crossing point and the phase along the upper adiabatic potential $E_2(x)$, and are given explicitly by

$$p = \exp\left[-\frac{\pi}{4\sqrt{\alpha\beta}} \left(\frac{2}{1+(1-\beta^{-2}f)^{1/2}} \right)^{1/2} \right], \tag{2.3}$$

$$\psi = \sigma - \phi_S - g, \tag{2.4}$$

with

$$\phi_S = \frac{\delta}{\pi}\ln\left(\frac{\delta}{\pi} \right) - \frac{\delta}{\pi} - \arg\Gamma\left(i\frac{\delta}{\pi} \right) - \frac{\pi}{4}, \tag{2.5}$$
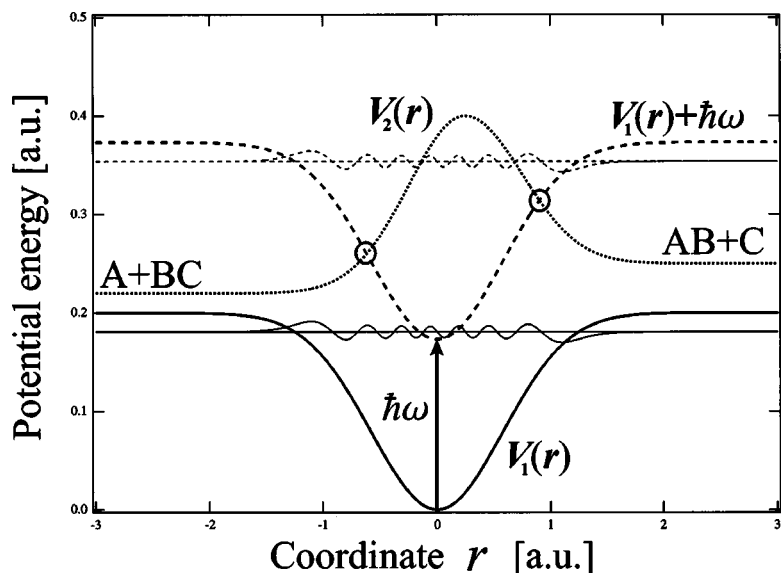
FIG. 2. One-dimensional model of the control scheme. Solid line: ground electronic state $V_1(r)$, dotted line: the excited electronic state $V_2(r)$. Two circles represent the NT type crossings created between the excited electronic state and the dressed ground electronic state (dashed line). The 14th vibrational eigenstate (thin line) and its dressed state (thin dashed line) of $V_1(r)$ are also depicted.

$$\sigma = \int_{t_1}^{t_2} k_2(x) dx, \tag{2.6}$$

$$g = \frac{0.23\alpha^{1/4}}{\alpha^{1/4}+0.75} 40^{-\sigma}, \tag{2.7}$$

$$f = 0.72 - 0.62\alpha^{0.715}, \tag{2.8}$$

$$\delta = \frac{\pi}{16\sqrt{\alpha\beta}} \frac{(6+10\sqrt{1-\beta^{-2}})^{1/2}}{1+\sqrt{1-\beta^{-2}}}, \tag{2.9}$$

$$\alpha = \frac{(1-\gamma^2)\hbar^2}{m(x_b-x_t)^2(E_b-E_t)}, \tag{2.10}$$

$$\beta = \frac{E-(E_b+E_t)/2}{(E_b-E_t)/2}, \tag{2.11}$$

$$\gamma = \frac{E_b-E_t}{E_2\left(\dfrac{x_b+x_t}{2}\right)-E_1\left(\dfrac{x_b+x_t}{2}\right)}, \tag{2.12}$$

and

$$k_j(x) = \frac{\sqrt{2m(E-E_j(x))}}{\hbar}. \tag{2.13}$$

The function $\Theta(x)$ is a step function defined by

$$\Theta(x) = \begin{cases} 0 & \text{for } x<0 \\ 1 & \text{for } x>0 \end{cases},$$

$E_1(x)$ $(E_2(x))$ is the lower (upper) adiabatic potential. $x_t(x_b)$ and $E_t(E_b)$ are the position of the top (bottom) of the lower (upper) adiabatic potential and the energy at $x_t(x_b)$. t_1 and t_2 are the turning points on $E_2(x)$ at energy E. m is the mass of a transmitting particle.

As is easily seen from Eq. (2.1), the complete reflection $(|T|^2=0)$ occurs at discrete energies which satisfy

$$\psi = (n+\tfrac{1}{2})\pi \quad (n=0,1,2,3,...). \tag{2.14}$$

This phenomenon can be interpreted as the quantum-mechanical interference effect between the transmitting wave

which simply crosses the barrier along the lower adiabatic potential without any transition to the upper adiabatic potential and the transmitting wave which is trapped by the upper adiabatic potential. At the energies of complete reflection, these waves interfere destructively at the exit whatever the nonadiabatic transition probability p is, and the incident wave is completely reflected back. In a periodic potential system we can utilize this complete reflection phenomenon together with the complete transmission to propose a new model of molecular switching.[20–22] By somehow changing some of the potential units in the array so that the condition of complete reflection is satisfied, switching of transmission can be realized.

Here we try to use this phenomenon to control molecular photodissociation. Taking a simple one-dimensional model of a triatomic molecule ABC consisting of a bound ground electronic state and a dissociative excited electronic state with two dissociation channels A+BC and AB+C, we demonstrate our idea. We first prepare an appropriate vibrationally excited state in the ground electronic state. Then we apply a stationary laser field with the laser frequency ω. This laser dresses up the ground electronic state by the photon energy $\hbar\omega$ and the NT type avoided crossings are created in the two dissociative channels, A+BC and AB+C (see Fig. 2). By adjusting the laser frequency ω, we can create the complete reflection condition in either one of the two dissociation channels, that is to say, we can switch off the corresponding dissociation channel and let the molecule dissociate into the other channel. This cannot be realized, however, with the ground vibrational state, because the corresponding phase ψ is not enough to satisfy Eq. (2.14).

With use of the semiclassical theory, we can further clarify the above-mentioned control scheme analytically. It is convenient to use the following transfer matrix N which belongs to the $SU(1,1)$ Lie group and connect the coefficients A, B, C, and D of the wave functions on both sides of the crossing as follows [see Fig. 1(a)]:[20,21]

$$\begin{pmatrix} C \\ D \end{pmatrix} = N \begin{pmatrix} A \\ B \end{pmatrix}, \tag{2.15}$$
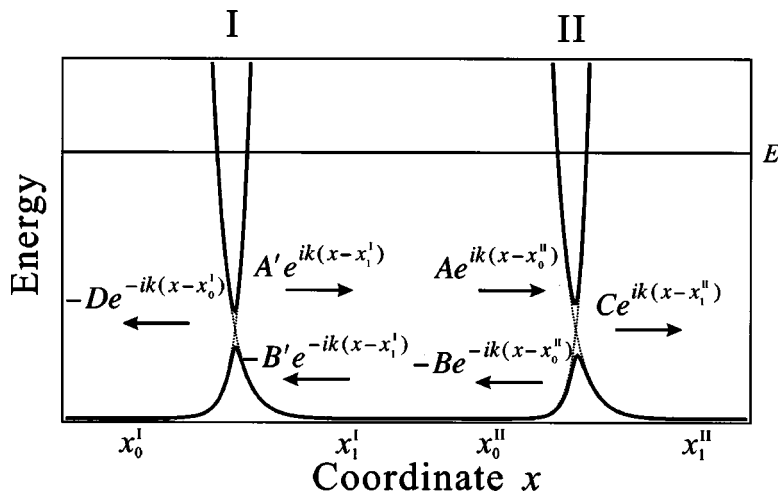
FIG. 3. Two units of the NT type crossing potentials. The left-side (right-side) unit is refered to as I (II). Solid (dotted) line: adiabatic (diabatic) potential. Potentials for $x \le x_0^{\mathrm{I}}$, $x_1^{\mathrm{I}} \le x \le x_0^{\mathrm{II}}$, and $x \ge x_1^{\mathrm{II}}$ are assumed to be flat. The barrier in the middle is taken to be high enough so that the tunneling there can be neglected.

where

$$N = \begin{pmatrix} \dfrac{1}{T^*} & \dfrac{R^*}{T^*} \\ \dfrac{R}{T} & \dfrac{1}{T} \end{pmatrix}.$$ (2.16)

Here $R \equiv |R|e^{i\delta_R}$ represents the reflection amplitude and is given by

$$|R| = \sqrt{1 - |T|^2},$$ (2.17)

and

$$\delta_R = -\frac{\pi}{2} + 2 \int_{x_0}^{x_t} k_1(x)dx + 2 \int_{x_b}^{t_2} k_2(x)dx + 2\sigma_0$$

$$- \tan^{-1}\left[\frac{(1-p)\sin(2\psi)}{1+(1-p)\cos(2\psi)}\right],$$ (2.18)

where T, p, and ψ are given before, and

$$\sigma_0 = \frac{x_b - x_t}{2}\left\{k_1(x_t) + k_2(x_b) + \frac{1}{3}\frac{[k_1(x_t) - k_2(x_b)]^2}{k_1(x_t) + k_2(x_b)}\right\}.$$ (2.19)

Now let us consider the two NT-type of curve crossings shown in Fig. 3, where the potential barrier in the middle is assumed to be high enough for the tunneling to be negligible. Suppose we prepare an initial wave in the middle, and no incoming waves from outside of the system. Then we have the following equations:

$$\begin{pmatrix} C \\ 0 \end{pmatrix} = N_{\mathrm{II}}\begin{pmatrix} A \\ B \end{pmatrix},$$ (2.20)

$$\begin{pmatrix} A' \\ B' \end{pmatrix} = N_{\mathrm{I}}\begin{pmatrix} 0 \\ D \end{pmatrix},$$ (2.21)

$$\begin{pmatrix} A \\ B \end{pmatrix} = \begin{pmatrix} e^{ikl} & 0 \\ 0 & e^{-ikl} \end{pmatrix}\begin{pmatrix} A' \\ B' \end{pmatrix},$$ (2.22)

where $N_{\mathrm{I}}(N_{\mathrm{II}})$ represents the N matrix at the left (right) side curve crossing, and is given by [see Eq. (2.16)]

$$N_j = \begin{pmatrix} \dfrac{1}{T_j^*} & \dfrac{R_j^*}{T_j^*} \\ \dfrac{R_j}{T_j} & \dfrac{1}{T_j} \end{pmatrix} \quad (j = \mathrm{I}, \mathrm{II}).$$ (2.23)

The quantities k and l are, respectively, the wave number at zero potential in the middle and the distance $x_0^{\mathrm{II}} - x_1^{\mathrm{I}}$ between the two units.

From Eqs. (2.20)–(2.22), we have

$$B = -R_{\mathrm{II}}A = \frac{1}{R_1^*}e^{-2i(\delta_T + kl)}A,$$ (2.24)

$$C = T_{\mathrm{II}}A,$$ (2.25)

and

$$D = \frac{T_{\mathrm{I}}^*}{R_{\mathrm{I}}^*}e^{-ikl}A.$$ (2.26)

If we want to stop the dissociation into the right side and make the molecule dissociate completely into the left side, i.e., $C = 0$, then we naturally obtain the following condition from Eq. (2.25):

$$T_{\mathrm{II}} = 0.$$ (2.27)

What is required is an appropriate choice of the laser frequency and the initial vibrational state to satisfy the complete reflection condition at the right side NT type crossing. Similarly, if we want to dissociate the molecule completely into the right side, $D = 0$, then we have to satisfy the condition,

$$T_{\mathrm{I}} = 0,$$ (2.28)

which is satisfied at different laser frequencies from those of Eq. (2.26). Thus, by appropriately adjusting the laser frequency, we can switch on and off the dissociation as we desire. When the conditions (2.27) and (2.28) are satisfied at the same time, the initial wave is trapped in between the two potential units and bound states in the continuum can be created. This is possible when the two potential units are the same and the condition of quantization is satisfied.[21]

J. Chem. Phys., Vol. 113, No. 15, 15 October 2000

Laser control of photodissociation   6201

Vardi and Shapiro[24] proposed an idea of laser catalysis in which an electronically ground state with a potential barrier has two crossings with a well type excited state in the dressed state picture and complete suppression of tunneling occurs. Depending on the parameters, the complete reflection and transmission coexist at energies very close to each other, indicating that this is a special case of the Fano-type resonance.[24,25] Interestingly, this phenomenon can be analyzed analytically by the Zhu–Nakamura theory also.[26] The complete reflection phenomenon in this case is induced by the two curve crossings and is quite different from the present one which occurs at one unit of the NT type curve crossing. The present one is more versatile, since the complete reflection can be controlled independently from the complete transmission.

III. SWITCHING OF PHOTODISSOCIATION IN ONE-DIMENSIONAL MODEL

In order to demonstrate the present idea clearly, numerical calculations of wave packet propagation are carried out for a one-dimensional potential system shown in Fig. 2. The potential functions employed are

$$V_1(r) = 0.2(1 - e^{-1.5r^2}),\tag{3.1}$$

$$V_2(r) = \begin{cases} 0.15e^{-2.0(r-0.25)^2} + 0.25 \ (r > 0.25) \\ 0.18e^{-2.0(r-0.25)^2} + 0.22 \ (r \leq 0.25) \end{cases}\tag{3.2}$$

in atomic units. The molecule-laser interaction is taken to be

$$V_{\text{int}}(t) = -\mu E(t) = \mu \sqrt{I} \cos(\omega t + \delta),\tag{3.3}$$

where μ is the transition dipole moment between the two electronic states and $E(t)$ is the stationary laser field with the frequency ω and the intensity I. The one-dimensional time-dependent Schrödinger equation to be solved is

$$i\hbar \frac{\partial}{\partial t} \begin{bmatrix} \Psi_1(r,t) \\ \Psi_2(r,t) \end{bmatrix}$$
$$= \begin{bmatrix} -\frac{\hbar^2}{2m}\frac{d^2}{dr^2} + V_1(r) & -\mu E(t) \\ -\mu E(t) & -\frac{\hbar^2}{2m}\frac{d^2}{dr^2} + V_2(r) \end{bmatrix}$$
$$\times \begin{bmatrix} \Psi_1(r,t) \\ \Psi_2(r,t) \end{bmatrix},\tag{3.4}$$

where $\Psi_1(r,t)$ ($\Psi_2(r,t)$) is the nuclear wave function on the ground (excited) electronic state. Eq. (3.4) is solved by using the split operator method[27] with the fast Fourier transform:

$$\begin{bmatrix} \Psi_1(r,t+\Delta t) \\ \Psi_2(r,t+\Delta t) \end{bmatrix} = \exp\left(-\frac{i}{\hbar}\frac{\hat{V}}{2}\Delta t\right) \exp\left(-\frac{i}{\hbar}\hat{K}\Delta t\right)$$
$$\times \exp\left(-\frac{i}{\hbar}\frac{\hat{V}}{2}\Delta t\right) \begin{bmatrix} \Psi_1(r,t) \\ \Psi_2(r,t) \end{bmatrix} + o(\Delta t^3),\tag{3.5}$$

where $\hat{V}$ and $\hat{K}$ are the 2×2 matrices,

$$\hat{V} = \begin{bmatrix} V_1(r) & -\mu E(t) \\ -\mu E(t) & V_2(r) \end{bmatrix},\tag{3.6}$$

$$\hat{K} = \begin{bmatrix} -\frac{\hbar^2}{2m}\frac{d^2}{dr^2} & 0 \\ 0 & -\frac{\hbar^2}{2m}\frac{d^2}{dr^2} \end{bmatrix}.\tag{3.7}$$

The dissociation flux is integrated over time at a certain asymptotic position to obtain the corresponding dissociation probability. In order to prevent the unphysical reflection of the wave packet at the edges, the negative imaginary potential (absorption potential) is put at both ends.[28] We have prepared the 14th vibrational eigenstate of the ground electronic state (the quantum number $v = 13$) as an initial state and used the following parameters for the wave packet calculation: m (reduced mass) $= 1.0$ a.m.u., $\mu = 1.0$ a.u., $I = 1.0$ TW/cm^2, Δt (time step) $= 1.0$ a.u., and Δr (spatial grid size) $= 0.016$ a.u.. The total number of the spatial grid points is 512.

The complete reflection positions can be analytically predicted as is shown in Fig. 4(a). Once the laser intensity I is selected, the shapes of the adiabatic potential curves, i.e., the ground electronic state shifted up by one photon energy $V_1(r) + \hbar\omega$ and the excited electronic state $V_2(r)$, are determined for a fixed laser frequency ω and then the positions of complete reflection can be easily estimated by solving Eq. (2.14). The solid (dashed) line in Fig. 4(a) represents the complete reflection position at the left-side (right-side) channel. The dotted line represents the relevant vibrational level, which is shifted up by one photon energy $\hbar\omega$, namely a linear function of the frequency ω. Thus the crossing points marked by solid (dotted) circles give the positions of the complete reflection for this vibrational state on the left (right) side. The calculated dissociation probabilities against laser frequency are depicted in Fig. 4(b). In order to concentrate on the important dissociation dynamics, here, we have assumed that the initial vibrational state was prepared. The solid (dotted) line represents the dissociation into the right (left) channel; the zero probability positions of the solid (dotted) line coincide with the solid (dotted) circles in Fig. 4(a). The highest dip at $\omega \sim 48\,000$ cm^{-1} is not complete because of tunneling. Wave packet dynamics are shown in Fig. 5 for the laser frequencies corresponding to (a) the complete reflection on the right side ($\omega = 31\,000$ cm^{-1}) and (b) the complete reflection on the left ($\omega = 35\,000$ cm^{-1}). The ground state component $|\Psi_1|^2$ which represents the initial eigenstate at $t = 0$ decays as time goes, while the excited state component $|\Psi_2|^2$ completely moves out into the left (right) dissociation channel, A+BC (AB+C), as seen in Figs. 5(a) and 5(b).

As is demonstrated above, within the one-dimensional model our control scheme can be perfect and a molecule can be made to dissociate into any channel as we desire by adjusting the laser frequency for a given vibrational state. The initial vibrational state should, however, be appropriately an excited one, since the phase ψ should satisfy Eq. (2.14).

(a)

(b)
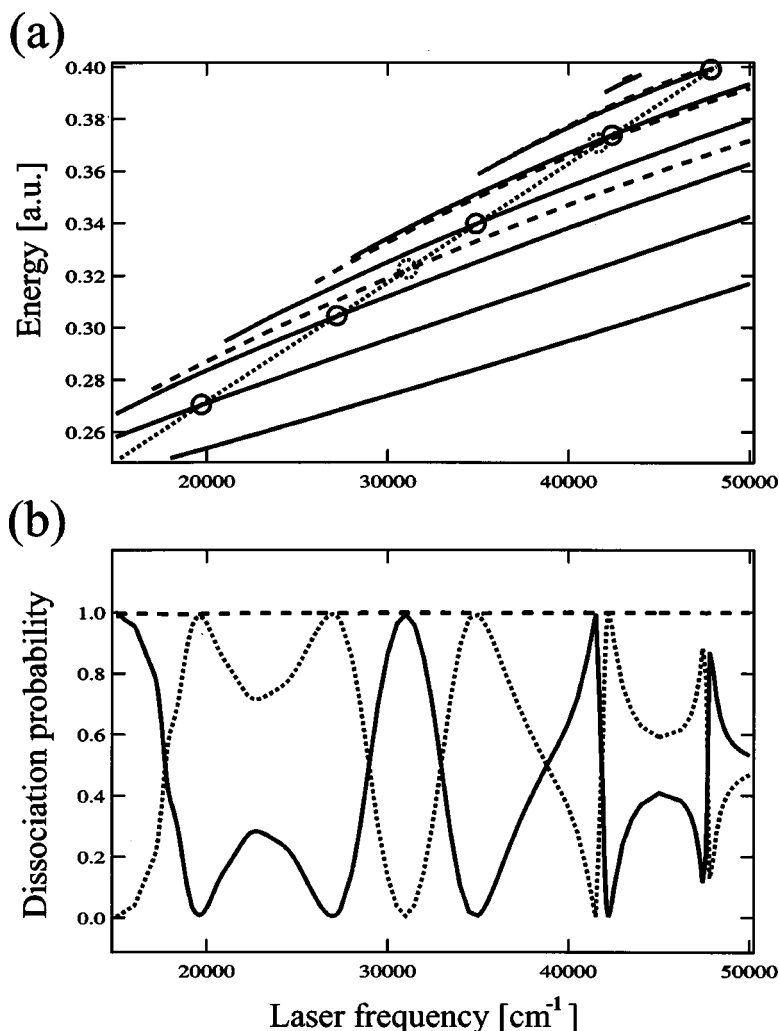
FIG. 4. (a) Analytical prediction of the complete reflection positions. Solid (dashed) lines: complete reflection positions at the left-side (right-side) channel. Dotted line: the dressed 14th vibrational eigen state of $V_1(r)$. Solid (dashed) circles represent the complete reflection of the vibrational state at the left-side (right-side) crossing. (b) Dissociation probability as a function of laser frequency. Solid line: dissociation into the right-side (AB+C) channel, dotted line: dissociation into the left-side (A+BC) channel, dashed line: sum of the two dissociation probabilities to guarantee the unitarity.

IV. CONTROL OF MOLECULAR PHOTODISSOCIATION IN TWO-DIMENSIONAL MODEL

A. Switching of photodissociation

Let us next consider a two-dimensional model. As an example, we take the HOD molecule with two dissociation channels: H+OD and HO+D. We consider the ground electronic state $\widetilde{X}$ and the excited electronic state $\widetilde{A}$. The bending and rotational motions are neglected for simplicity with the bending angle fixed at the equilibrium structure of the ground electronic state, i.e., at 104.52 deg. The ground electronic state potential $V_1(r_H,r_D)$ [shown by dotted lines in Fig. 6(a)] is taken to be two coupled Morse oscillators,[29]

$$V_1(r_H,r_D)=D(1-e^{-\gamma(r_H-r_0)^2})+D(1-e^{-\gamma(r_D-r_0)^2})$$

$$-B\frac{(r_H-r_0)(r_D-r_0)}{1+e^{A((r_H-r_0)+(r_D-r_0))}}, \qquad (4.1)$$

where $r_H(r_D)$ represents the H–O (D–O) bond length, and $D=0.2092$ hartree, $\gamma=1.1327$ a.u.$^{-1}$, $r_0=1.81$ a.u., $A=3.0$ a.u.$^{-1}$, and $B=0.25$ hartree/a.u.^{2}. The last term repre-

sents the mode coupling, and the parameters A and B are assumed to be larger than the values used in Ref. 29 ($A=1.0$ a.u.$^{-1}$ and $B=0.006\,76$ hartree/a.u.^{2}) in order to demonstrate the present control scheme more clearly. The excited electronic state $V_2(r_H,r_D)$ shown in Fig. 6(b) is taken to be the analytical function of Engel et al.,[30] which was fitted to the ab initio calculations by Staemmler et al..[31] The mass-scaled Jacobi coordinates r for O–H distance and R for OH–D distance are introduced,

$$r=\left(\frac{m_{OH}}{m_{D,OH}}\right)^{1/4}|\mathbf{r}_H|, \qquad (4.2)$$

$$R=\left(\frac{m_{D,OH}}{m_{OH}}\right)^{1/4}\left|\mathbf{r}_D-\frac{m_H}{m_H+m_O}\mathbf{r}_H\right|, \qquad (4.3)$$

where $\mathbf{r}_H(\mathbf{r}_D)$ is the vector from O atom to H (D) atom, $m_{OH}=m_O m_H/(m_O+m_H)$, $m_{D,OH}=[m_D(m_O+m_H)]/(m_D+m_O+m_H)$, and m_H, m_O, and m_D are the mass of H, O, and D, respectively. With use of these coordinates (r,R) the two-dimensional time-dependent Schrödinger equation is written as
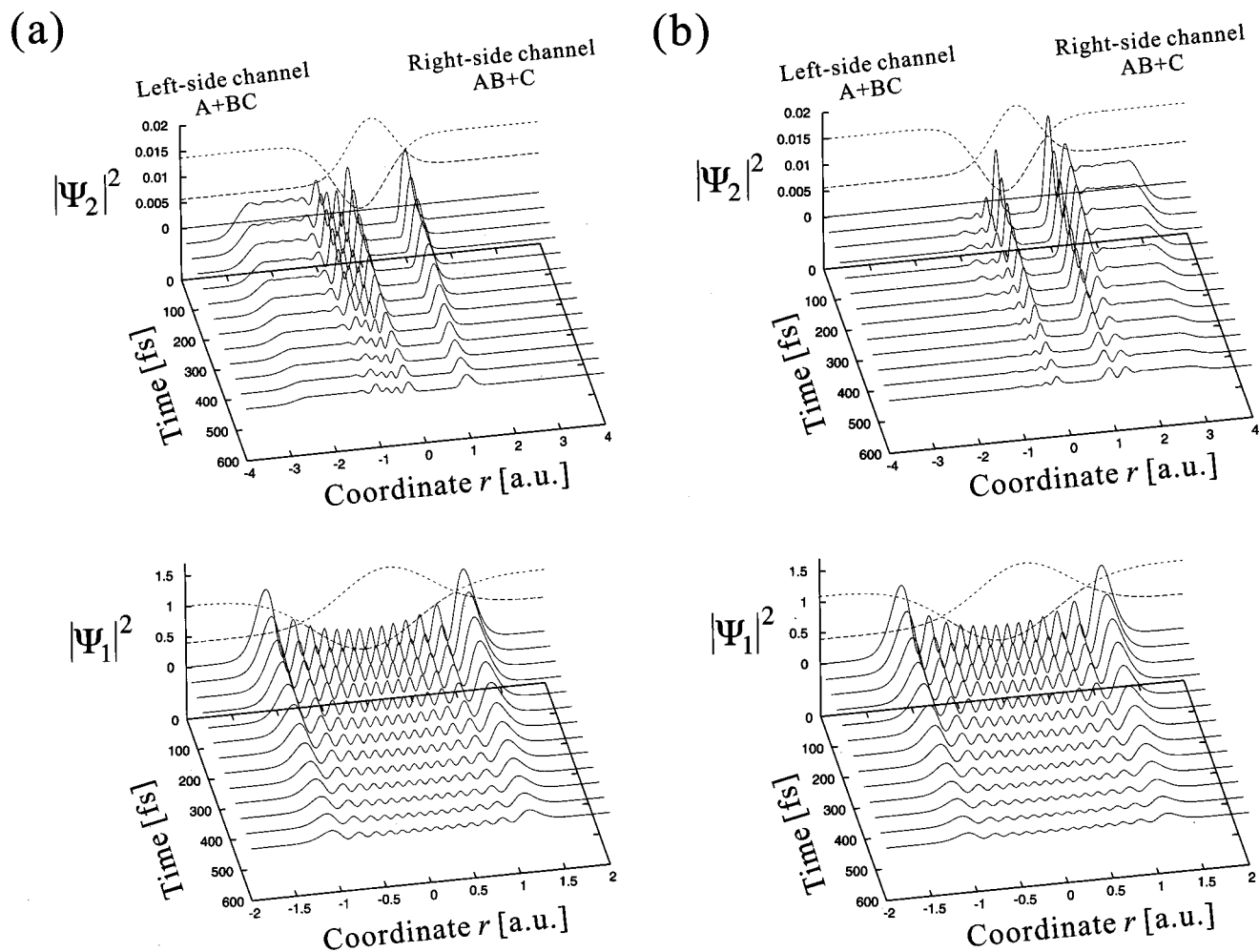
FIG. 5. Time-dependent dynamics of wave packet when the laser frequency is (a) 31 000 cm^{-1} and (b) 35 000 cm^{-1}. The upper (lower) part of each figure shows the dynamics of the excited (ground) state wave packet (solid line). The dotted (dashed) line represents the upper (lower) adiabatic potential.

$$
i\hbar \frac{\partial}{\partial t}\begin{bmatrix}\Psi_1(r,R,t)\\ \Psi_2(r,R,t)\end{bmatrix} = \begin{bmatrix} -\dfrac{\hbar^2}{2m}\left(\dfrac{\partial^2}{\partial r^2}+\dfrac{\partial^2}{\partial R^2}\right)+V_1(r,R) & -\mu E(t) \\[2ex] -\mu E(t) & -\dfrac{\hbar^2}{2m}\left(\dfrac{\partial^2}{\partial r^2}+\dfrac{\partial^2}{\partial R^2}\right)+V_2(r,R)\end{bmatrix}\times\begin{bmatrix}\Psi_1(r,R,t)\\ \Psi_2(r,R,t)\end{bmatrix}. \tag{4.4}
$$

Here m is the reduced mass of the system,

$$
m=\sqrt{\frac{m_H m_O m_D}{m_H+m_O+m_D}}. \tag{4.5}
$$

$\Psi_1(r,R,t)$ ($\Psi_2(r,R,t)$) represents the wavefunction of the ground (excited) electronic state. Equation (4.4) is solved by using the split operator method with the two-dimensional fast Fourier transform in the same way as in Sec. III. The dissociation flux is integrated over time in a certain asymptotic region before the negative imaginary potentials which are put at both ends. The transition dipole moment μ is assumed to be 1.0 a.u. and the stationary laser field $E(t)$ is taken to be $\sqrt{I}\cos(\omega t+\delta)$. An initial state is prepared at the 145th vibrational eigenstate of $V_1(r,R)$ by solving the two-dimensional eigenvalue problem by the DVR (discrete variable representation) method.[32] This initial state is mainly

composed of the 17th vibrational state of the O–H bond and the 23rd vibrational state of the O–D bond and spreads into both bonds due to the coupling, as is depicted by solid lines in Fig. 6(a). The laser intensity I and the various grid sizes are taken to be 1.0 TW/cm^2, $\Delta t=1.0$ a.u., $\Delta r=0.029$ a.u., and $\Delta R=0.034$ a.u., respectively. The total number of the spatial grid points is 256×256. Figure 7(a) depicts the calculated dissociation probabilities against laser frequency. The solid (dotted) line represents the dissociation probability into the H+OD (HO+D) channel. The dissociation probabilities change alternatively as a function of the laser frequency ω, and the dissociation into the H+OD (HO+D) channel is preferential when the laser frequency ω is ~7000, 8000, 10 000, and 11 500 cm^{-1} (9000, 11 000, and 14 000 cm^{-1}). The control is not perfect this time because of multidimensionality, but is still quite selective. The molecule can

(a)

(b)
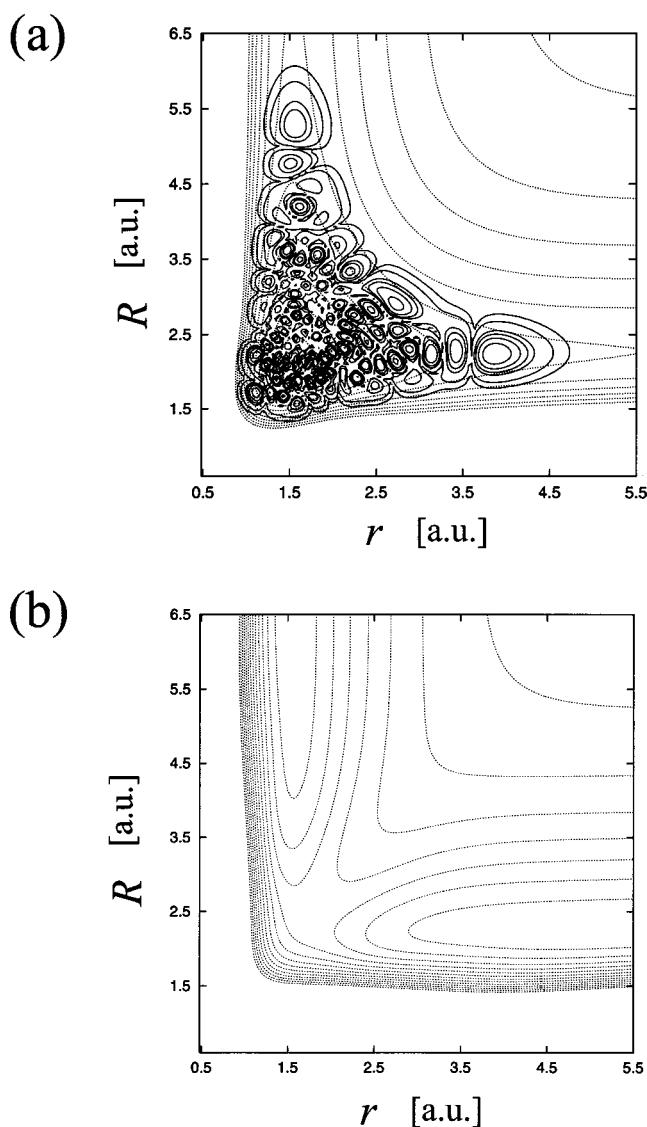
FIG. 6. (a) Contour plots of the ground electronic state of HOD (dotted line). The contour spacing is 8500 cm^{-1}. The density of the 145th vibrational eigenstate is superimposed (solid line). (b) Contour plots of the excited electronic state of HOD. The contour spacing is 5000 cm^{-1}.

be made to dissociate preferentially into any channel as we desire by choosing the laser frequency and the vibrational state appropriately. The complete reflection positions in the H+OD (HO+D) channel can be roughly estimated analytically by taking a one-dimensional cut of the potential energy surface along the minimum energy path of the O–H (O–D) bond into account and using the one-dimensional formula Eq. (2.14). The vibrational state is taken to be $v=17(23)$ for the O–H (O–D) channel. Figure 7(b) depicts these estimates. The solid (dashed) lines represent the complete reflection positions in the H+OD (HO+D) channel. The dotted (dash–dotted) line shows the vibrational state $v=17$ of the O–H bond ($v=23$ of the O–D bond) shifted up by one photon energy. Thus the solid (dotted) circles indicate the positions of complete reflection in the H+OD (HO+D) channel. As is seen in Fig. 7(a), the dips of calculated dissociation probabilities correspond well to the complete reflection positions predicted analytically. Exceptions are the dip at ω

~ 7200 cm^{-1} and the peak at $\omega \sim 13\,500$ cm^{-1} in the H+OD dissociation channel. The former is shallow and shifted to higher frequency (~ 7500 cm^{-1}) in Fig. 7(a), and the latter has almost disappeared. This is due to the topography of the potential energy surface, representing the difficulty of multi-dimensionality. The wave packet dynamics on the excited state are shown in Fig. 8. The wave packet is depicted by solid lines at various times. The dashed lines in these figures represent the crossing seam lines between the dressed ground state and the excited state. Figure 8(a) corresponds to the laser frequency 9000 cm^{-1}, and thus the wave packet moves out into the HO+D channel. Figure 8(b) corresponds to the laser frequency 11 500 cm^{-1}, and the wave packet almost dissociates into the H+OD channel [see Fig. 7(a)].

As the above results demonstrate, the selective dissociation based on the complete reflection phenomenon can be realized even in two-dimensional systems. The control naturally cannot be perfect like in the one-dimensional case, but can still be quite effective. The dissociation into a certain channel is stopped by the complete reflection phenomenon and the reflected wave packet is transfered into the other channel due to the mode-coupling via the ground electronic state and is finally dissociated into the latter channel. No analytical theory exists for two-dimensional problems, but the one-dimensional theory can be used to some extent in the above-mentioned way to roughly estimate the appropriate conditions. The favorable conditions of the selective control in the two-dimensional system may be summarized as follows: The mode-coupling in the ground electronic state should be localized around the equilibrium position and should be negligible in the region of crossing seam created by the laser field. Otherwise the mode-coupling potential destroys the complete reflection condition. In other words, the initial vibrational state should have the one mode character around the region of crossing seam, and the L-shape wave function like that in Fig. 6(a) is favorable.

B. Dissociation into non-dissociative channel

Our control scheme can also be applied to such a two-dimensional system that the excited electronic state has a potential barrier which is shifted very much to one of the channels and prohibits the dissociation into that channel. As such a model system, we have employed the same potentials as those used in the previous subsection and slightly modified the excited state potential so that the saddle point is located in the HO+D channel (see Fig. 9). The only one term of the excited electronic state, $0.244\,358\,9\times10^{2}$ $\times(S_1S_3^2+S_1^2S_3)$ in Ref. 30, is changed to $0.144\,358\,9\times10^{2}$ $\times(S_1S_3^2+0.8S_2^2S_3)$. With this modification the dissociation into the HO+D channel is not possible anymore along the excited state potential surface, if the initial vibrational state is localized in the H+OD channel. The same initial state and method of wave packet propagation are used as those in the previous subsection. The calculated dissociation probabilities against the laser frequency are shown in Fig. 10(a). The solid (dotted) line stands for the dissociation probability into the H+OD (HO+D) channel. When the laser frequency is either one of $\sim 10\,000$ cm^{-1}, $\sim 12\,500$ cm^{-1}, $\sim 17\,000$ cm^{-1}, and

(a)

(b)

Laser frequency [cm^{-1}]
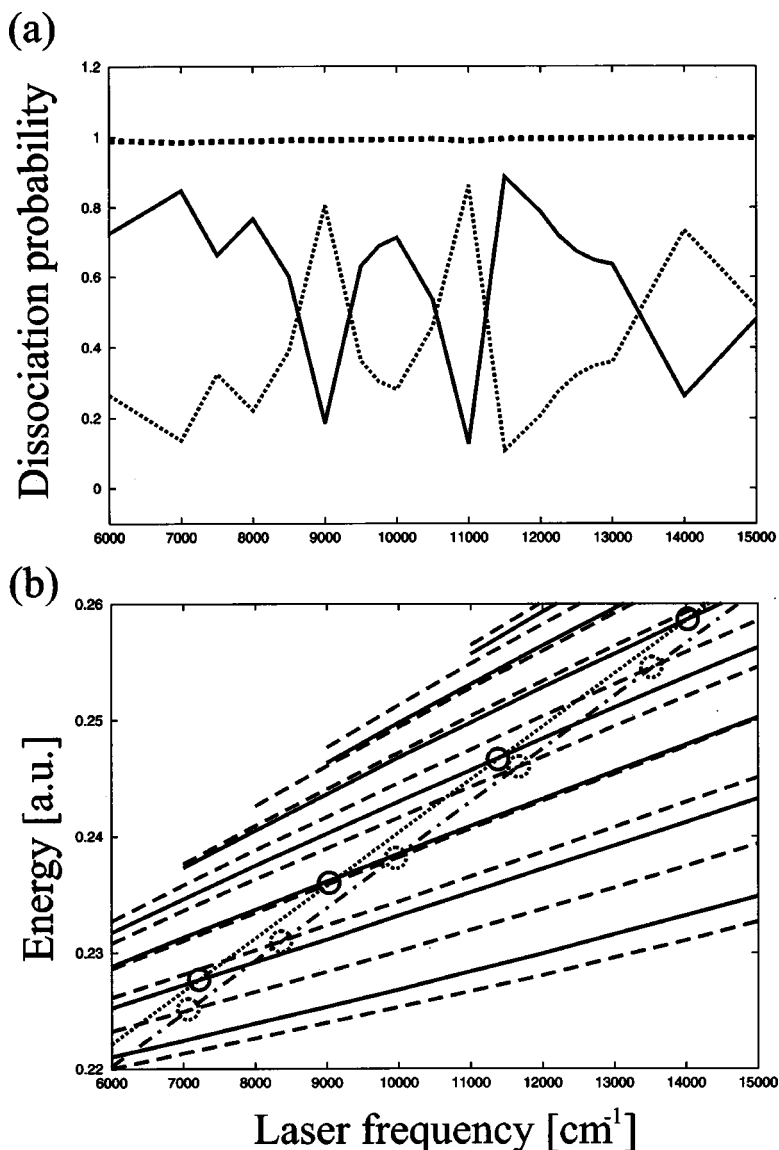
FIG. 7. (a) Dissociation probability against laser frequency in the case of the 145th vibrational state of HOD. Solid (dotted) line: dissociation into the H+OD(HO+D) channel. Dashed line: sum of the two dissociation probabilities. (b) Analytical prediction of the complete reflection positions. Solid (dashed) lines: the complete reflection positions in the H+OD(HO+D) channel. Dotted (dash–dotted) line: the vibrational state $v=17$ of the O–H bond ($v=23$ of the O–D bond). The solid (dotted) circles represent the complete reflection positions when the 145th vibrational eigenstate is prepared as an initial state on the H+OD(HO+D) side.

$\sim$19 000 cm^{-1}, the dissociation into the H+OD channel is preferential, while the dissociation into the HO+D channel is preferential when the laser frequency is set at $\sim$9000 cm^{-1}, $\sim$11 000 cm^{-1}, or $\sim$13 500 cm^{-1}. As is clearly seen, the control is quite selective and the dissociation even into the non-dissociative HO+D channel is possible by adjusting the laser frequency appropriately. The analytical prediction of the complete reflection positions is shown in Fig. 10(b) in the same way as in Fig. 7. The solid (dashed) lines depict the complete reflection positions in the H+OD(HO+D) channel, and the dotted (dash–dotted) line represents the vibrational state $v=17$ of the O–H bond ($v=23$ of the O–D bond) shifted up by one photon energy. The solid (dotted) circles show the position of the complete reflection in the H+OD(HO+D) channel. The dissociation probability dips in Fig. 10(a) coincide quite well with these analytical predictions. Some of the dips ($\omega \sim 16\,000$ cm^{-1} and 18 000 cm^{-1}) and the peak at $\omega \sim 15\,000$ cm^{-1} are, however, not complete because of the multi-dimensional topography of potential energy surface.

The CH$_3$SH molecule resembles the model studied in this subsection in the sense that the saddle point of the excited electronic state is located in the CH$_3$+SH channel and blocks the C–S bond breaking.[33] This molecule is actually known not to be dissociated into this channel by the ordinary photodissociation. The similar type of two-dimensional wave packet calculations are performed with use of the potential energy surfaces available in the literature.[33] The initial vibrational state used is the 123rd one which corresponds to the $v=8$ local mode of the S–H bond. In the same way as before, Fig. 11(a) presents the analytical prediction of the complete reflection positions in the CH$_3$S+H channel based on the one-dimensional cut of the potential energy surface along the minimum energy path of the S–H bond and the vibrational state $v=8$ of the S–H bond. Figure 11(b) shows the dissociation flux accumulated over the time interval of 1 ps for the S–H bond breaking, i.e., the dissociation into the CH$_3$S+H channel, as a function of the laser frequency. There are some conspicuous dips which correspond to the circles in Fig. 11(a). These dips are, of course, due to the complete reflection in the CH$_3$S+H channel and indicate that the reflected wave packet can be transferred into the other channel

(a)

(b)
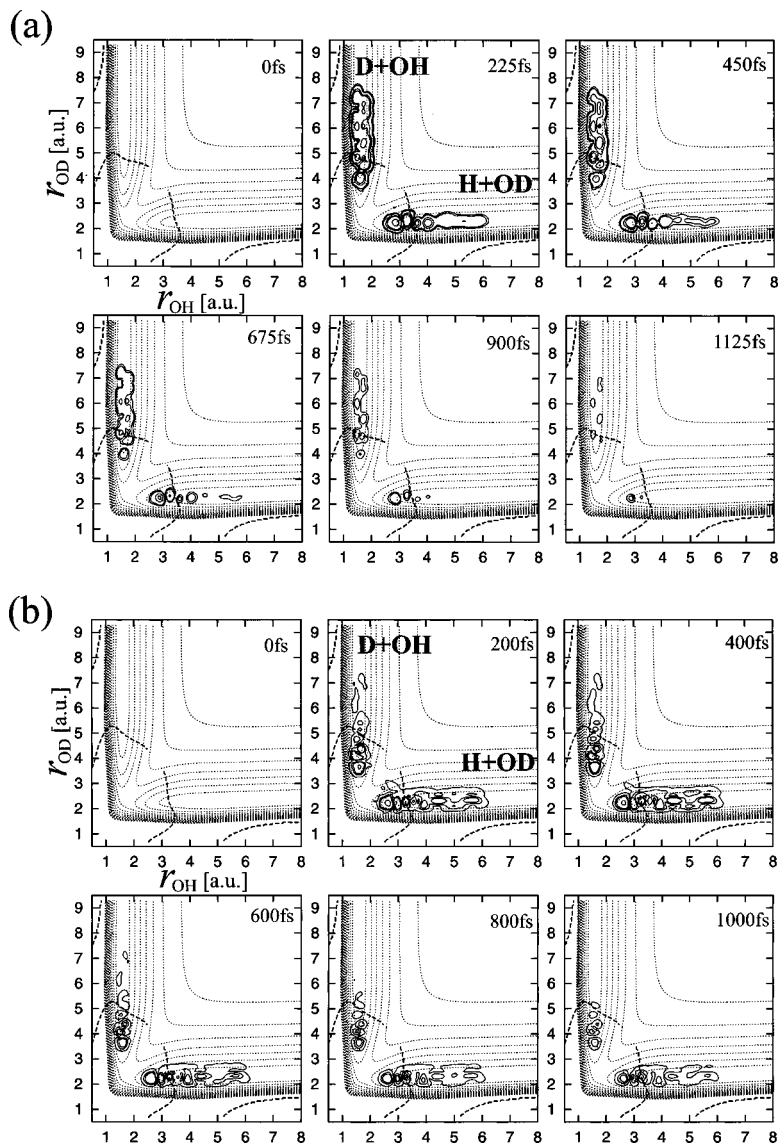
FIG. 8. Time-dependent behavior of the excited state wave packet for the laser frequency (a) 9000 cm^{-1} and (b) 11 500 cm^{-1} (the contours of the density by solid line). The contours of the excited electronic state are superimposed (dotted line). The dashed lines represent the crossing seams induced by the laser field.

CH$_3$+SH via the ground electronic state through the mode-coupling. In the present model potential, however, there is no mode-coupling between the two channels in the ground electronic state; thus the wave packet stays inside and does not dissociate into the CH$_3$+SH channel. If there were an appropriate coupling between the two channels, we could dissociate this molecule into the unusual channel of CH$_3$+SH by using the present control scheme.

V. CONCLUDING REMARKS

In this paper, a new control scheme of molecular photodissociation with use of the complete reflection phenomenon was proposed and demonstrated numerically in the one- and two-dimensional models. In the present control scheme, an appropriate vibrational excited state is prepared at first and then by applying the stationary laser field with the laser frequency ω the two NT type avoided crossings are created between the ground electronic bound state dressed up by one photon energy $\hbar\omega$ and the excited dissociative electronic state. If the complete reflection occurs at the NT type curve crossing in one channel, that channel is switched off and the
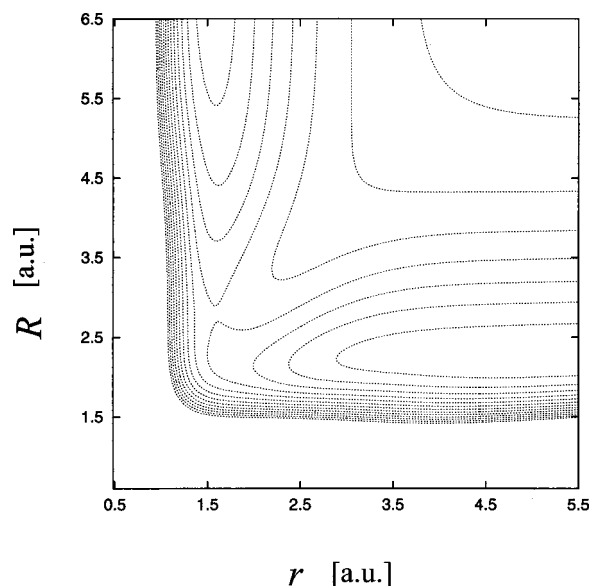
FIG. 9. Contour plots of the modified excited electronic state of HOD. The saddle point is located in the HO+D channel. The contour spacing is 5000 cm^{-1}.

(a)

(b)

Laser frequency [cm^{-1}]
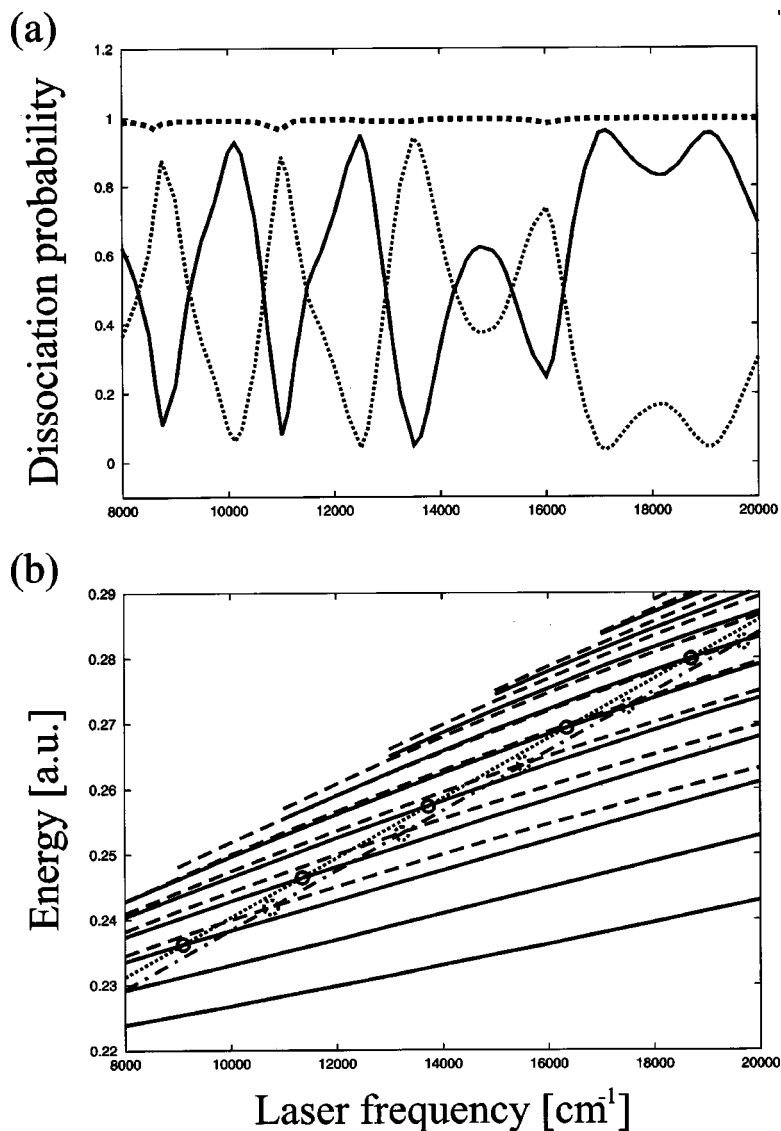
FIG. 10. (a) Dissociation probability against laser frequency in the case of the 145th vibrational state of HOD. Solid (dotted) line: dissociation into the H+OD(HO+D) channel. Dashed line: sum of the two dissociation probabilities. (b) Analytical prediction of the complete reflection positions. Solid (dashed) lines: the complete reflection positions in the H+OD(HO+D) channel. Dotted (dash–dotted) line: the vibrational state $v=17$ of the O–H bond ($v=23$ of the O–D bond). The solid (dotted) circles represent the complete reflection positions for the 145th vibrational eigenstate.

dissociation into the other channel becomes preferential. By adjusting the laser frequency, we can create the complete reflection condition at any one of the two dissociation channels, and thus we can selectively switch on and off the dissociation. Within the one-dimensional model this scheme can be completely realized. In the two-dimensional models, the control cannot be complete because of multidimensionality, but can still be effective and selective, as was demonstrated with use of the model mimicking the HOD molecule. The selective dissociation even into a non-dissociative channel is demonstrated to be possible. Good points of the present new control scheme may be summarized as follows:

(1) Stationary laser field is good enough and only the frequency is required to be adjusted.
(2) Strong laser field is not necessarily needed and the present scheme is not very sensitive to small fluctuation of the laser intensity I, because the complete reflection position is mainly dependent on the laser frequency and is much less dependent on the laser intensity. The sensitivity to the laser frequency becomes less at lower intensity. This is because the complete reflection dip becomes

wider for the weaker diabatic coupling, i.e., for the weaker laser intensity, although the transmission on the other side becomes a bit less effective.[16,17,19]

(3) The control can be selective because of the complete reflection phenomenon. The wave which is reflected at one NT type curve crossing due to the complete reflection is transferred via the ground electronic state and dissociated into the other channel by the mode-coupling potential.
(4) Selective dissociation can be made even into such a non-dissociative channel that cannot be attained in the usual photodissociation method because of a potential barrier in the excited electronic state.
(5) Analytical prediction of the complete reflection positions can be easily made with use of the one-dimensional semiclassical theory and the appropriate selection of initial state and laser frequency can be carried out analytically. Even in a two-dimensional model such analytical prediction can be performed to a good extent with use of the one-dimensional theory, when the initial vibrational state has local mode character in the region of the cross-

(a)

(b)

Laser frequency [cm^{-1}]
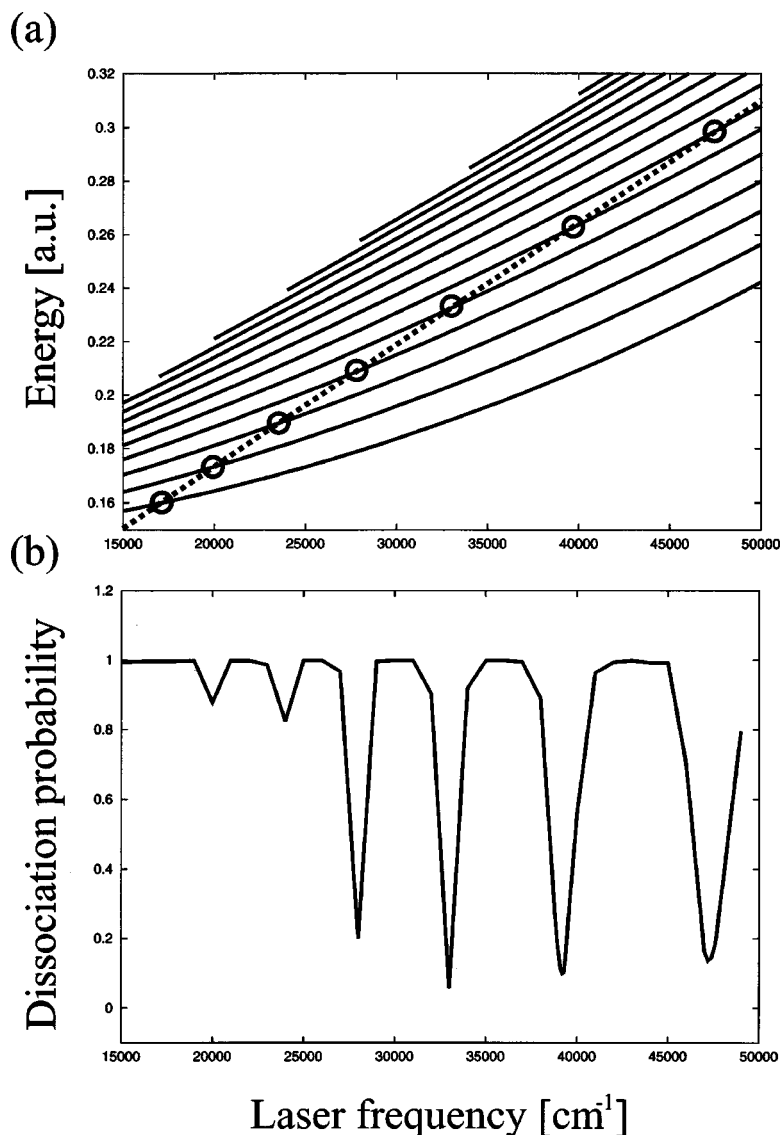
FIG. 11. (a) Analytical prediction of the complete reflection positions in the case of two-dimensional model of CH_3SH. Solid line: the complete reflection positions in the CH_3S+H channel. Dashed line: the vibrational state $v=8$ of the S–H bond. The solid circles represent the complete reflection positions for the 123rd vibrational eigenstate. (b) Dissociation probability against the laser frequency for $CH_3SH \rightarrow CH_3S+H$ in the case of the 123rd vibrational state.

ing seam created by the laser field, i.e., when the mode coupling is localized away from the crossing seam. These are the favorable conditions for the selective control in two-dimensional cases.

Defects of the present scheme, on the other hand, are that the scheme is quite sensitive to potential energy surface topography, especially in high-dimensional systems and that a vibrationally excited state is necessary to be prepared as an initial state. Another problem which is not essential but should be taken into account in practical applications is position dependence of the transition dipole moment.

The present control scheme cannot be very robust, because the method is based on the phase interference; but this can present a new intriguing selective control of molecular photodissociation when the conditions with respect to potential energy surface topography and initial vibrational state are appropriately satisfied. The use of the hyperspherical coordinate system may be useful to analyze the multi-dimensional case more clearly. This will be reported in a future publication.

The complete reflection phenomenon can happen in

some other potential crossing systems as reported in Ref. 26 and those cases can also be used to control some other type of molecular processes.

ACKNOWLEDGMENTS

[1] R. J. Gordon and S. A. Rice, Annu. Rev. Phys. Chem. **48**, 601 (1997).
[2] A. D. Bandrauk, *Molecules in Laser Fields* (Marcel Dekker, New York, 1994).
[3] P. Brumer and M. Shapiro, Annu. Rev. Phys. Chem. **43**, 257 (1992).
[4] D. J. Tannor and S. A. Rice, J. Chem. Phys. **83**, 5013 (1985).
[5] R. Kosloff, S. A. Rice, P. Gaspard, S. Tersigni, and D. J. Tannor, Chem. Phys. **139**, 201 (1989).
[6] D. Neuhauser and H. Rabitz, Acc. Chem. Res. **26**, 496 (1993).
[7] B. Kohler, J. L. Krause, F. Raksi, K. R. Wilson, V. V. Yakovlev, and R. M. Whitnell, Acc. Chem. Res. **28**, 133 (1995).
[8] M. Sugawara and Y. Fujimura, J. Chem. Phys. **100**, 5646 (1994).
[9] S. Chelkowski and A. D. Bandrauk, J. Chem. Phys. **99**, 4279 (1993).
[10] M. M. T. Loy, Phys. Rev. Lett. **32**, 814 (1974).

[11] J. S. Melinger, S. R. Gandhi, and W. S. Warren, J. Chem. Phys. **101**, 6439 (1994).

[12] S. Guerin, Phys. Rev. A **56**, 1458 (1997).

[13] K. Mishima and K. Yamashita, J. Chem. Phys. **109**, 1801 (1998).

[14] Y. Teranishi and H. Nakamura, Phys. Rev. Lett. **81**, 2032 (1998).

[15] Y. Teranishi and H. Nakamura, J. Chem. Phys. **111**, 1415 (1999).

[16] H. Nakamura, *Dynamics of Molecules and Chemical Reactions*, edited by R. E. Wyatt and J. Z. H. Zhang (Marcel Dekker, New York, 1996), p. 473.

[17] H. Nakamura and C. Zhu, Comments At. Mol. Phys. **32**, 249 (1996).

[18] S. I. Chu, *Advances in Multiphoton Processes and Spectroscopy, Vol. 2* (World Scientific, Singapore, 1986).

[19] C. Zhu and H. Nakamura, J. Chem. Phys. **97**, 1892 (1992); **97**, 8497 (1992); **98**, 6208 (1993); **101**, 4855 (1994); **101**, 10630 (1994); **102**, 7448 (1995); **107**, 7839 (1997).

[20] H. Nakamura, J. Chem. Phys. **97**, 256 (1992).

[21] S. Nanbu, H. Nakamura, and F. O. Goodman, J. Chem. Phys. **107**, 5445 (1997).

[22] H. Nakamura, J. Chem. Phys. **110**, 10253 (1999).

[23] C. Zhu, Y. Teranishi, and H. Nakamura, Adv. Chem. Phys. (to be published).

[24] A. Vardi and M. Shapiro, Phys. Rev. A **58**, 1352 (1998).

[25] U. Fano, Phys. Rev. **124**, 1866 (1961).

[26] L. Pichl, H. Nakamura, and J. Horacek, J. Chem. Phys. **113**, 906 (2000).

[27] C. Leforestier, R. H. Besseling, C. Cerjan *et al.*, J. Comput. Phys. **94**, 59 (1991).

[28] Á. Vibók and G. G. Balint-Kurti, J. Chem. Phys. **96**, 7615 (1992).

[29] J. R. Reimers and R. O. Watts, Mol. Phys. **52**, 357 (1984).

[30] V. Engel, R. Shinke, and V. Staemmler, J. Chem. Phys. **88**, 129 (1988).

[31] V. Staemmler and A. Palma, Chem. Phys. **93**, 63 (1985).

[32] J. C. Light, I. P. Hamilton, and J. V. Lill, J. Chem. Phys. **82**, 1400 (1985).

[33] J. E. Stevens, H. W. Jang, L. J. Butler, and J. C. Light, J. Chem. Phys. **102**, 7059 (1995).